Transboundary water challenges and potential collaboration

in the Tigris-Euphrates river basin water management

Alla Golub*
golub@purdue.edu

Iman Haqiqi*
ihaqiqi@purdue.edu

Omid Karami**
okarami@purdue.edu

Ehsanreza Sajedinia**
esajedin@purdue.edu

Farzad Taheripour*
tfarzad@purdue.edu

*Center for Global Trade Analysis, Department of Agricultural Economics, Purdue University
** Department of Agricultural Economics, Purdue University

Selected Paper prepared for presentation at the 2022 Agricultural and Applied Economics Association Annual Meeting, Anaheim, CA, July 31-August 2.

Draft not for quotation and citation

Transboundary water challenges and potential collaboration in the Tigris-Euphrates river basin water management

Introduction

Today, 47 percent of the global population live in areas that suffer water scarcity at least one month each year, and by 2050 this share will increase to 57 percent (UNESCO 2018). Globally, transboundary rivers carry almost 60% of freshwater flows and are crucial in ensuring people have an adequate water supply (Economist Intelligence Unit 2020). These shared resources need to be managed in a sustainable, equitable, and collaborative manner. Of the seven transboundary river systems ranked by how well countries manage transboundary water resources, the Tigris-Euphrates river basin has the lowest score (Economist Intelligence Unit 2020). The two rivers and their tributaries run mainly through Turkey, Syria, Iraq, and Iran. Turkey has the largest reserves of renewable water among these countries and control over the flow to the downstream countries due to the construction of dams (Shamout and Lahn 2015). The situation in the basin is particularly difficult due to climate change, weak cooperation among riparian countries, intensive hydropower development, inefficient agricultural practices, and political instability (Shamout and Lahn 2015). Ongoing construction of dams and hydropower plants and projected increase in water needs in Turkey are major concerns in the downstream countries, particularly in Iraq and Syria. At the same time, by midcentury climate change may result in a 20 percent reduction in rainfall over the river basin (IPCC 2013) and the availability of water for irrigation may decline by 13-28 percent (Haqiqi 2019).

This study has several objectives. First, it evaluates the impacts of climate change on water scarcity in the Tigris-Euphrates and other river basins within the Middle East region under

alternative climate futures and translates ensuing changes in water supply into economic outcomes. Then, it evaluates the economic outcomes of transboundary water allocation scenarios and considers cooperation plans that can be implemented to reduce controversies over water allocation in the Tigris-Euphrates river basin. In addition to the contribution to resource policy literature, this study offers a unique coupling of a complex economic model with a hydrological model. This research extends the earlier analysis in Taheripour et al. (2020) by estimating changes in water availability with a hydrological model, and by analyzing new scenarios of water allocation and agreements among countries in the region.

Methodology

Economic model

The economic analysis is implemented using a comparative static computable general equilibrium model GTAP-BIO-W that combines economic and biophysical information on land and water at the spatial resolution of River Basin–Agro-Ecological Zone (RB-AEZ) in each region of the model (Liu et al. 2014; Taheripour, Hertel, and Liu 2013; Taheripour et al., 2018). Iran, Iraq, Jordan, Lebanon, Syria, Saudi Arabia, and Turkey are separate regions in the model. Other countries are grouped into the Rest of the Middle East and the Rest of the World regions. The time horizon of the analysis is the middle of the 21st century. The framework is designed to examine the nexus between agricultural activities and trade in the presence of climate change and water scarcity by country and on a global scale. In this version of the GTAP-BIO-W model, water is modeled as an explicit input in irrigated agriculture, livestock, and water utility services, with the latter supplying water to other sectors and the final demand in the model. The three activities compete for water at the river basin level, while individual crops compete for water

within RB-AEZ. Irrigated crops are distinguished from rainfed. A large river basin could serve several AEZs. Thus, water consumption is traced by sector and country at the river basin level by AEZ.

Hydrological model

Changes in the natural water runoff of the river basins of the region, including but not limited to the Tigris-Euphrates river basin, due to climate change and changes in water withdrawals are quantified using a hydrological model based on the Water Balance Model (WBM) (Haqiqi 2019). WBM (Vörösmarty, Federer, and Schloss 1998; D. Grogan 2016), originally developed at the University of New Hampshire, is a global model that simulates both the vertical exchange of water between the ground and the atmosphere and the horizontal transport of water through runoff and stream networks at the grid cell level. The model separates surface water and groundwater. It considers location-specific parameters and projects the available surface water and groundwater considering precipitation, irrigation volume, evapotranspiration, and flow routing. The hydrological model determines the annual supply of water at the 15 arc-min grid cell level based on: 1) climate scenarios, 2) the main parameters of WBM, and 3) consumption allocation of water among countries for agricultural and non-agricultural uses. Given the harvested area, which is exogenous in the model, the model produces irrigation requirements to maintain agricultural yields in future climate, and how this requirement is met by withdrawals from surface water (SW), shallow groundwater (GW), and deep or unsustainable groundwater (UGW). Deep groundwater for irrigation is more expensive than the surface and shallow groundwater due to higher pumping costs and becomes even more expensive as the water table

goes down. The increase in deep groundwater use for irrigation or other uses serves as a proxy for surface and shallow groundwater scarcity.

The spatial scope of this study is concentrated on the river basins of the region with major attention to the Tigris-Euphrates river basin and the neighboring countries. The temporal dimension is from 2016 to 2050 to reflect the current and future conditions. The changes in water supply aggregated from 15 arc-min grid cells to river basin and country are inputs in the economic analysis with GTAP-BIO-W. The shocks to water supply, representing water scarcity in the economic model, are calculated as a negative of increase in deep groundwater withdrawal relative to the total water withdrawal in the initial period, where the total includes withdrawals of surface, shallow underground, and deep underground water (see appendix C for details).

Climate change scenarios

Two climate scenarios considered in the analysis are RCP8.5 and RCP4.5. Daily temperature and precipitation variables are critical inputs in the hydrological model to project the availability of water resources in the future. We use two data sources in parallel to obtain projections of these two variables. The first data source is NASA Earth Exchange Global Daily Downscaled Projections (NEX-GDDP-CMIP6) (Thrasher, B. et al. 2021; 2022). The NEX-GDDP-CMIP6 dataset is comprised of downscaled climate scenarios for the globe that are derived from the General Circulation Model (GCM) runs conducted under the Coupled Model Intercomparison Project Phase 6. The Bias-Correction Spatial Disaggregation (BCSD) method used to generate the NEX-GDDP-CMIP6 dataset is a statistical downscaling algorithm developed to address limitations of global GCM outputs, such as coarse resolution grids and locally biased projections in their statistical characteristics when compared with observations. The dataset compiles climate projections from thirty-five CMIP6 GCMs and four SSP scenarios (SSP2-4.5, SSP5-8.5, SSP1-

2.6, and SSP3-7.0) for the period from 2015 to 2100. In this analysis, we use SSP2-4.5 and SSP5-8.5.

In addition to the NEX-GDDP-CMIP6 dataset, we also explore another climate dataset (Boyko, O., Reggiani, P., Todini, E. 2022) constructed using the methodology documented in (Reggiani et al. 2021). This data set is constructed using temperature and precipitation time series from 1979 to 2100 produced by 19 CMIP5 models for RCP8.5 and RCP4.5 climate scenarios. These series are mutually weighted and bias-corrected using ERA5 reanalysis data (Hersbach et al. 2020) from 1979 to 2005. This method yields unbiased and sharper predictive distributions for climatological variables in comparison to using the unprocessed ensemble distribution (Reggiani et al. 2021).

Temperature and precipitation variables representing two climate scenarios from the two climate products are inputted into the hydrological model to produce changes in soil moisture, groundwater, and surface water by 15 arcmin grid cells over the first half of this century. Thus, we will consider four sets of hydrological model outputs to inform the economic model about future water availability in the respective four baseline simulations.

Economic model scenarios

The first set of experiments quantifies the economic implications of climate change (Figure 1). The projections of future changes in precipitation and temperature are introduced into the hydrological model to determine future changes in the use of water for irrigation to maintain agricultural yields due to water stress, keeping harvested area and non-agricultural water uses fixed at the levels observed in the base year of the analysis.

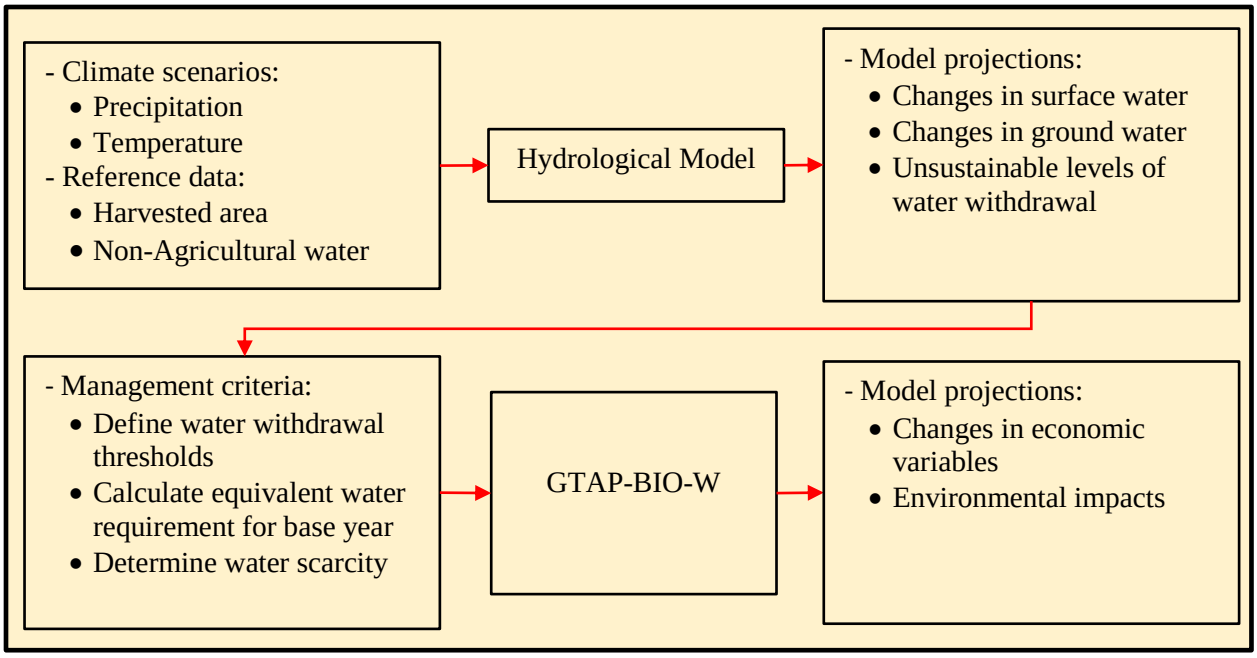

Figure 1. Baseline scenarios

The hydrological model projects changes in SW, GW, and UGW withdrawals by river basin in all countries of the Middle East region, including but not limited to the Tigris-Euphrates river basin. Using the hydrological model projections, we determine water scarcity shocks by river basin and region/country. These water scarcity measures representing a reduction in the water supply are introduced into the CGE model to determine the economic and environmental impacts of climate change for each baseline scenario.

The second set of scenarios combines climate impacts with increases in upstream countries' water withdrawals (mainly Turkey) and reduced water availability in the downstream countries within the Tigris-Euphrates RB (Shamout and Lahn 2015). These simulations allow for the evaluation of different water allocation plans in the region. The third set of scenarios evaluates potential agreements among countries that aim to redistribute gains and losses due to water withdrawals. The scenarios consider general-purpose monetary transfers from upstream to downstream countries, as well as transfers to subsidize food consumption and transfers to pay for

improvements in water use efficiency (WUE). The improvements in WUE require more capital inputs in agricultural sectors and may offset the negative impact of reduced water supply on food production in downstream countries. Finally, we will explore scenarios of cooperation in water management among riparian countries. The current version of the paper only highlights the results for climate scenario RCP8.5 mentioned above.

Preliminary results based on climate scenario RCP8.5

Reduction in water supply projected by hydrological model

The simplified Water Balance Model (Haqiqi 2019) takes the conditions of the state variables in the initial period. The state variables are the water stored in different forms and locations at one point in time. This includes volumetric soil moisture levels in mm, shallow groundwater depth in mm, reservoir storage in m3, and initial snowpack in mm. These conditions are calculated following (D. S. Grogan et al. 2022) based on MERRA-2 observations (Randles et al. 2017). Figure 2 illustrates the average reservoir storage in the Tigris-Euphrates river basin and the larger Middle East region simulated by the model given current climate conditions.

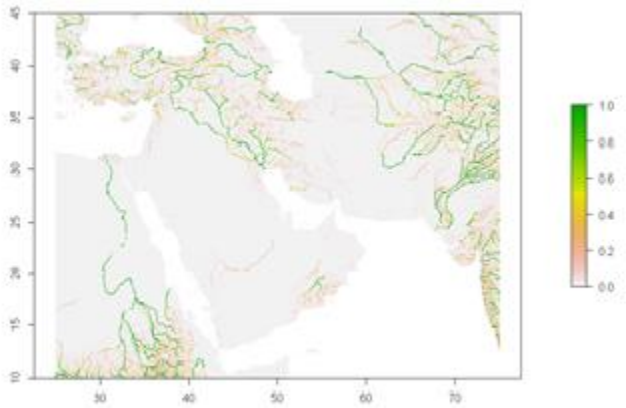

Figure 2. Average monthly reservoir storage up to 1 million m3 over period from January 2012 to December 2018 in the Middle East region (units are in million m3).

The hydrological model runs are based on total daily precipitation (in mm/day) and near-surface daily average air temperature (in ℃) from the first day of 2016 to the last day of 2055. We use projected precipitation and temperature from two data sets. The first data set is NEX-GDDP-CMIP6 which includes outputs of many GCM models. Ideally, we would like to run the hydrological model with each GCM output. However, this would require very large computing resources. Instead, we choose just one GCM model, MIROC-ES2L, from the NEX-GDDP-CMIP6 dataset (the selection process is described in Appendix A). Precipitation for selected countries based on the daily output of the MIROC-ES2L model with SSP5-8.5 climate is shown in Figure A12 in Appendix. Turkey receives more precipitation than other countries in the region, and this will continue, though with some downward trend for all countries. The second data set is a climate data product (Boyko, O., Reggiani, P., Todini, E. 2022) constructed using temperature and precipitation projected by 19 CMIP5 GCMs and the methodology in Reggiani et al. (2021). We will refer to the second data set as an ensemble.

Reductions in water supply by river basin and country constructed using hydrological model output are presented in Figure 3. A comparison of the hydrological model results using MIROC-ES2L vs. the ensemble as an input reveals that projected reductions in water supply and variance across countries and river basins are larger with the single model MIROC-ES2L. The differences are especially large for Iran and Turkey. With MIROC-ES2L projections, the hydrological model predicts that Iran will experience the largest relative reduction in water supply, reaching almost 40% in Western Asia Iran RB by 2050. Results based on the ensemble suggest that Turkey will experience the largest relative reduction of 12.6% in the Tigris-Euphrates RB. Overall, results based on MIROC-ES2L and the ensemble agree that Iran, Turkey, and Iraq will experience larger relative reductions in water supply than other countries and the

Rest of the Middle East region considered in the analysis. Also, results based on the MIROC-ES2L and the ensemble agree that in the Tigris-Euphrates RB the largest relative reduction in the water supply is projected in Turkey.

The reductions in the water supply are implemented in a comparative static GTAP-BIO-W CGE model to evaluate the economic implications of changes in water supply in the Middle East due to climate change. Note that in the model the reduced water availability affects only irrigated crops and gives an advantage to rainfed crops relative to irrigated. Another effect of climate change on both irrigated and rainfed crops is changes in yields. To represent the impacts of climate change on crop yields, we implement changes in total factor productivity (TFP) in rainfed and irrigated crop sectors used in Taheripour et al. (2020). For paddy rice, wheat, and coarse grains in the Middle East, TFP is reduced by 5% and 10% in irrigated and rainfed crops, respectively. For oilseeds and sugar crops, TFP is assumed to increase by 5% by 2050.

(A)

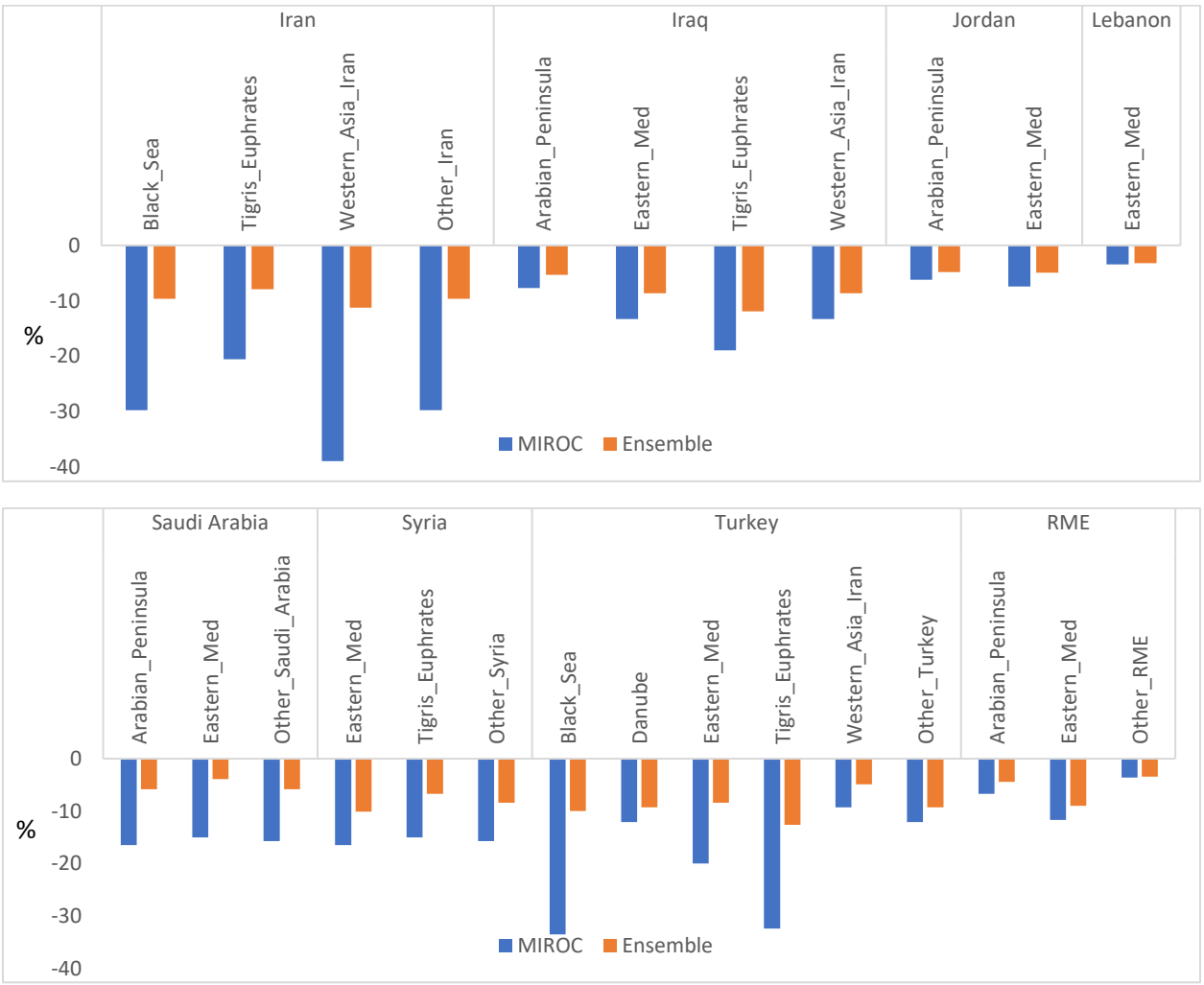

(B)

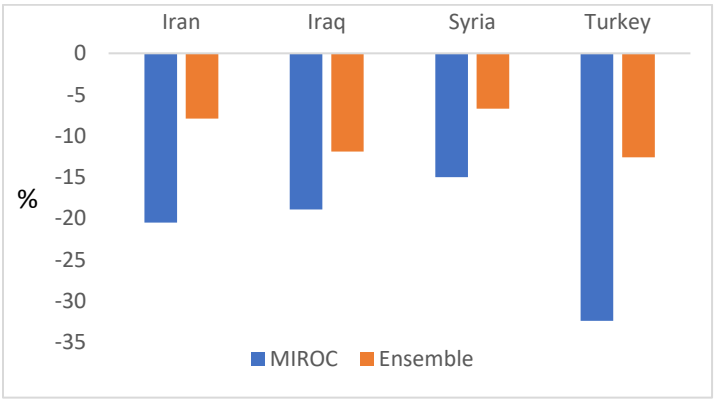

Figure 3. Reduction in water supply by 2050 by country and river basin, % change relative to current withdrawals. Panel A shows a reduction in water supply by country and river basin. Panel B shows a reduction in water supply in Tigris-Euphrates RB by country, the subset of panel A.

Impacts of climate change on water supply combined with changes in crop yields result in a reduction of GDP in the Middle East countries. As expected, reductions are larger when MIROC-ES2L projections are used as input in the hydrological model in comparison to ensemble input. The reductions are larger when water scarcity is combined with changes in crop yields, but most of the impact comes from water scarcity. In all four cases, Iran and Turkey experience the largest negative impacts on GDP. The share of agriculture in GDP is about 7% for Turkey and 10% for Iran. Large reductions in GDP in these countries are driven not only by impacts on agriculture but also impacts of water scarcity on industrial sectors.

Table 1. Changes in GDP in the Middle East due to reduction in water supply driven by RCP8.5 climate scenario with and without changes in crop yields, %

	Water scarcity		Water scarcity and changes in crop yields	
	MIROC	Ensemble	MIROC	Ensemble
Iran	-10.6	-2.8	-12.6	-4.7
Iraq	-3.7	-1.9	-4.1	-2.3
Jordan	-3.1	-1.5	-3.2	-1.5
Lebanon	-1.3	-0.7	-1.3	-0.7
Saudi	-0.5	-0.3	-0.5	-0.3
Syria	-7.4	-3.4	-8.1	-4.2
Turkey	-12.0	-4.5	-12.3	-4.8
RME	-2.0	-1.2	-2.1	-1.3

Water scarcity and water scarcity combined with changes in crop yields result in a reduction in crop output. The largest reductions in aggregate crop output are projected in Iraq and Turkey (Table 2). Among crop sectors, wheat sectors experience the largest negative impact, while the output of oilseeds is projected to expand in the RME region due to the assumed increase in yields (Table B1 in Appendix). Crop prices rise in all regions, with Turkey, Iran, and Iraq experiencing higher increases than other regions (Table 3). Crop imports by countries in the Middle East soar amid a reduction in domestic output. For example, paddy rice imports by Iraq increased by 50%

under the climate projections produced by the ensemble and more than doubled under the MIROC climate projections.

Table 2. Changes in aggregated crop output in the Middle East due to reduction in water supply driven by RCP8.5 climate scenario with and without changes in crop yields, %

	Water scarcity		Water scarcity and changes in crop yields	
	MIROC	Ensemble	MIROC	Ensemble
Iran	-8.0	-2.0	-9.9	-3.7
Iraq	-14.0	-8.7	-15.9	-10.8
Jordan	-0.6	-0.6	-0.7	-0.8
Lebanon	-1.6	-1.7	-1.7	-1.8
Saudi	-2.1	-2.0	-2.1	-1.9
Syria	-8.4	-4.1	-9.1	-4.9
Turkey	-19.8	-8.0	-20.2	-8.5
RME	-0.9	-0.8	-2.4	-2.3

Table 3 Changes in aggregate crop prices in the Middle East due to reduction in water supply driven by RCP8.5 climate scenario with and without changes in crop yields, %

	Water scarcity		Water scarcity and changes in crop yields	
	MIROC	Ensemble	MIROC	Ensemble
Iran	11.5	3.2	15.9	6.5
Iraq	19.3	10.8	21.8	13.2
Jordan	6.0	2.7	6.1	2.8
Lebanon	2.8	1.8	2.8	1.7
Saudi	3.6	2.4	3.7	2.5
Syria	9.0	4.0	10.1	5.1
Turkey	22.9	7.7	24.3	8.9
RME	1.9	1.0	2.7	1.7

Conclusions and next steps

The Middle East is one of the most water-scarce regions in the world. Due to climate change, population growth, unsustainable water management, economic growth, and ongoing conflicts, water scarcity in the region is likely to worsen (unicef.org). In particular, by the midcentury, the

region may experience a reduction in the availability of water for irrigation due to a reduction in rainfall.

Using projections of future temperature and precipitation under the RCP8.5 scenario and the hydrological model, we evaluated the impacts of climate change on water scarcity in the Tigris-Euphrates and other river basins within the Middle East region by 2050. We used two sources of future climate projections. The first source is the NEX-GDDP-CMIP6 data set from which we have chosen the output of the MIROC-ES2L model for the SSP5-8.5 scenario. The second source is the data set constructed using temperature and precipitation time series produced by 19 CMIP5 models for RCP8.5 (Boyko, O., Reggiani, P., Todini, E. 2022).

The hydrological model projects a large range of reductions in water supply in the Middle East region, between -3.2 and 38.9% by 2050, depending on the river basin and country. A comparison of the hydrological model results using MIROC-ES2L vs. the ensemble as an input reveals that projected reductions in water supply and their variance across countries and river basins are larger with MIROC. For example, when MIROC used as an input, Iran will experience a relative reduction in the water supply of almost 40% in Western Asia Iran RB by 2050. In both cases, MIROC and the ensemble, Iran, Turkey, and Iraq will experience larger relative reductions in water supply than other countries and the Rest of the Middle East region considered in the analysis. Within Tigris-Euphrates RB, the largest relative reduction in the water supply is projected in Turkey.

The reductions in water supply combined with assumptions regarding climate driven changes in crop yields are implemented in the comparative static CGE model to evaluate the economic impacts of these changes. Overall, the economic impacts of reduced water supply are much larger than the impacts from the assumed changes in crop yields. We find that Iran and

Turkey experience the largest negative impacts on GDP, about 12% in the MIROC case when both water scarcity and changes in crop yields are considered. These reductions in GDP are driven not only by impacts on agriculture but to a larger extent by the impacts of water scarcity on industrial sectors. Among crop sectors, wheat output experiences the largest negative impact. Crop imports by Middle East countries increase dramatically amid a reduction in domestic output.

The next steps in this work include an evaluation of the impacts of climate change on water scarcity under the RCP4.5 scenario. Then, we will combine climate impacts with increases in upstream countries' water withdrawals within Tigris-Euphrates RB. This will require additional runs with the hydrological model, driven by both projected temperature and precipitation and assumed increased withdrawals by the upstream countries. Finally, we will evaluate the economic outcomes of transboundary water allocation scenarios and consider cooperation plans that can be implemented to reduce controversies over water allocation in the Tigris-Euphrates river basin.

Acknowledgments

Climate scenarios used were from the NEX-GDDP-CMIP6 dataset, prepared by the Climate Analytics Group and NASA Ames Research Center using the NASA Earth Exchange and distributed by the NASA Center for Climate Simulation (NCCS).

We thank Alex Boyko, Paolo Reggiani, and Ezio Todini for constructing climate data product for the Middle East region using the methodology described in (Reggiani et al. 2021).

References

Abbasian, Mohammadsadegh, Sanaz Moghim, and Ahmad Abrishamchi. 2019. "Performance of the General Circulation Models in Simulating Temperature and Precipitation over Iran." *Theoretical and Applied Climatology* 135 (3–4): 1465–83. https://doi.org/10.1007/s00704-018-2456-y.

Boyko, O., Reggiani, P., Todini, E. 2022. *Temperature and Precipitation in the Middle East 1979-2100 Constructed Using CMIP5 Outputs*.

Economist Intelligence Unit. 2020. "The Blue Peace Index 2020."

Grogan, Danielle. 2016. "Global and Regional Assessments of Unsustainable Groundwater Use in Irrigated Agriculture." Doctoral Dissertations. University of New Hampshire. https://scholars.unh.edu/dissertation/2260.

Grogan, Danielle S., Shan Zuidema, Alex Prusevich, Wilfred M. Wollheim, Stanley Glidden, and Richard B. Lammers. 2022. "WBM: A Scalable Gridded Global Hydrologic Model with Water Tracking Functionality." Preprint. Hydrology. https://doi.org/10.5194/gmd-2022-59.

Haqiqi, Iman. 2019. "Irrigation, Water Scarcity, and Adaptation. Ph.D. Dissertation, Purdue University, West Lafayette, IN." Dissertation. Purdue University.

Hersbach, Hans, Bill Bell, Paul Berrisford, Shoji Hirahara, András Horányi, Joaquín Muñoz-Sabater, Julien Nicolas, et al. 2020. "The ERA5 Global Reanalysis." *Quarterly Journal of the Royal Meteorological Society* 146 (730): 1999–2049. https://doi.org/10.1002/qj.3803.

IPCC. 2013. "Climate Change 2013: The Physical Science Basis." In *Contribution of Working Group I to the Fifth Assessment Report of the Intergovernmental Panel on Climate Change*. Cambridge, United Kingdom and New York, NY, USA: Cambridge University Press.

Liu, Jing, Thomas W. Hertel, Farzad Taheripour, Tingju Zhu, and Claudia Ringler. 2014. "International Trade Buffers the Impact of Future Irrigation Shortfalls." *Global Environmental Change* 29 (November): 22–31. https://doi.org/10.1016/j.gloenvcha.2014.07.010.

McMahon, T. A., M. C. Peel, and D. J. Karoly. 2015. "Assessment of Precipitation and Temperature Data from CMIP3 Global Climate Models for Hydrologic Simulation." *Hydrology and Earth System Sciences* 19 (1): 361–77. https://doi.org/10.5194/hess-19-361-2015.

Randles, C. A., A. M. da Silva, V. Buchard, P. R. Colarco, A. Darmenov, R. Govindaraju, A. Smirnov, et al. 2017. "The MERRA-2 Aerosol Reanalysis, 1980 Onward. Part I: System Description and Data Assimilation Evaluation." *Journal of Climate* 30 (17): 6823–50. https://doi.org/10.1175/JCLI-D-16-0609.1.

Reggiani, Paolo, Ezio Todini, Oleksiy Boyko, and Roberto Buizza. 2021. "Assessing Uncertainty for Decision-making in Climate Adaptation and Risk Mitigation." *International Journal of Climatology* 41 (5): 2891–2912. https://doi.org/10.1002/joc.6996.

Shamout, Nouar, and Glada Lahn. 2015. "The Euphrates in Crisis: Channels of Cooperation for a Threatened River." Research Paper. Chatham House. https://www.chathamhouse.org/sites/default/files/field/field_document/20150413Euphrates_0.pdf.

Taheripour, Farzad, Thomas Hertel, and Jing Liu. 2013. “Introducing Water by River Basin into the GTAP-BIO Model: GTAP-BIO-W.” GTAP Working Paper 77. Department of Agricultural Economics, Purdue University, West Lafayette, IN: Global Trade Analysis Project (GTAP). https://www.gtap.agecon.purdue.edu/resources/res_display.asp?RecordID=4304.

Taheripour, Farzad, Thomas Hertel, Badri Narayanan, Sebnem Sahin, Anil Markandya, Bijon Kumer Mitra, and Vivek Prasad. n.d. “Climate Change and Water Scarcity: Growing Risks for Agricultural-Based Economies in South Asia.” In *Routledge Handbook of Sustainable Development in Asia*. 2018.

Thrasher, B., Wang, W., Michaelis, A., Melton, F., Lee, T., and Nemani, R. 2022. “NASA Global Daily Downscaled Projections, CMIP6.” Nature Scientific Data (in review).

Thrasher, B., Wang, W., Michaelis, A., and Nemani, R. 2021. “NASA Earth Exchange Global Daily Downscaled Projections - CMIP6.” NASA Center for Climate Simulation. https://doi.org/10.7917/OFSG3345.

UNESCO, ed. 2018. *Nature-Based Solutions for Water*. The United Nations World Water Development Report 2018. Paris: UNESCO.

Vörösmarty, C. J., C. A. Federer, and A. Schloss. 1998. “Potential Evaporation Functions Compared on U.S. Watersheds: Implications for Global-Scale Water Balance and Terrestrial Ecosystem Modeling.” *Journal of Hydrology* 207 (147–69).

Appendix A

While climate models have some agreement regarding temperature change, there is a large disagreement regarding precipitation. It is a standard practice to take a multi-model ensemble mean for temperature in the climate impact literature. However, the ensemble means for precipitation can be misleading due to the weak performance of some climate models regarding precipitation (McMahon, Peel, and Karoly 2015). We adopt Abbasian, Moghim, and Abrishamchi (2019) approach and evaluate CMIP5 GCMs in simulating precipitation over the Middle East to choose the best model. Cumulative annual, monthly, and seasonal precipitation metrics are calculated for each RB-AEZ within the Middle East region using GCMs model outputs and Modern-Era Retrospective Analysis for Research and Applications (MERRA-2) observational data from 1980 to 2005. Then, the correlation coefficient and root mean square error (RMSE) between each GCM and MERRA-2 are calculated for each cumulative metric.

We also developed extreme precipitation indices. The first index is the average length of the dry spell per growing period, where the dry spell is defined as consecutive days with precipitation less than 1 mm per day. The second index is the longest consecutive dry days per growing period. Again, correlation and RMSE are calculated for each GCM and MERRA-2 pair.

We find that all 20 CMIP5 models included in the analysis show very good performance when correlations are measured using all RB-AEZs. However, there is heterogeneity in performance across models when correlations are measured for each RB-AEZ separately. Many models perform poorly for a given RB-AEZ. Overall, all CMIP5 models perform well in simulating precipitation over the Middle East region on retrospective run. Models in the MIROC family, especially MIROC-ESM-CHEM, perform slightly better (but likely not significantly better statistically) (Figures A1-A11).

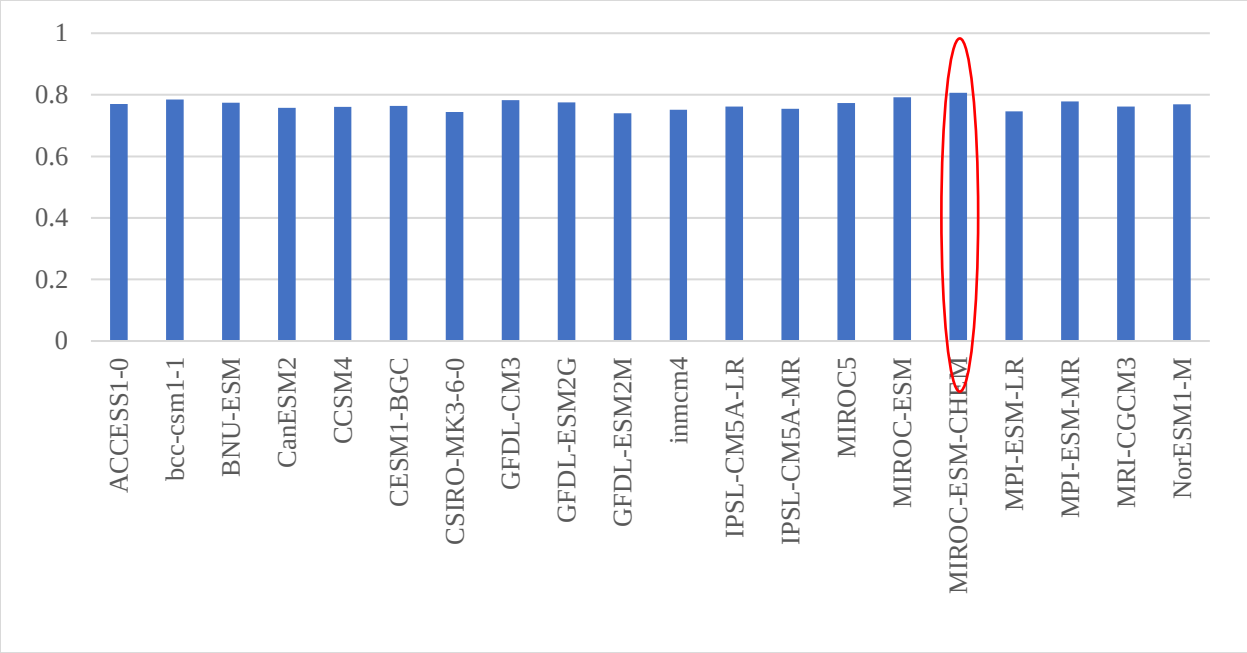

Figure A1. Annual precipitation correlations between historical observations and GCM output over 1980-2005 for the Middle East region.

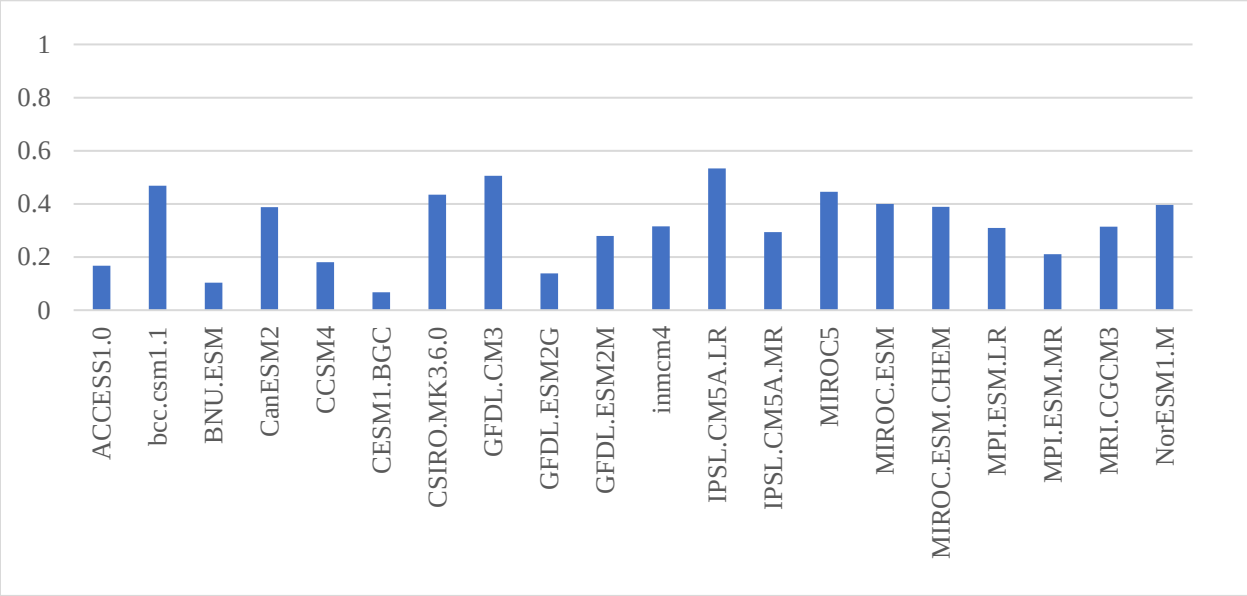

Figure A2. Annual precipitation correlations between historical observations and GCM output over 1980-2005 for Tigris-Euphrates RB in AEZ8 in Iraq.

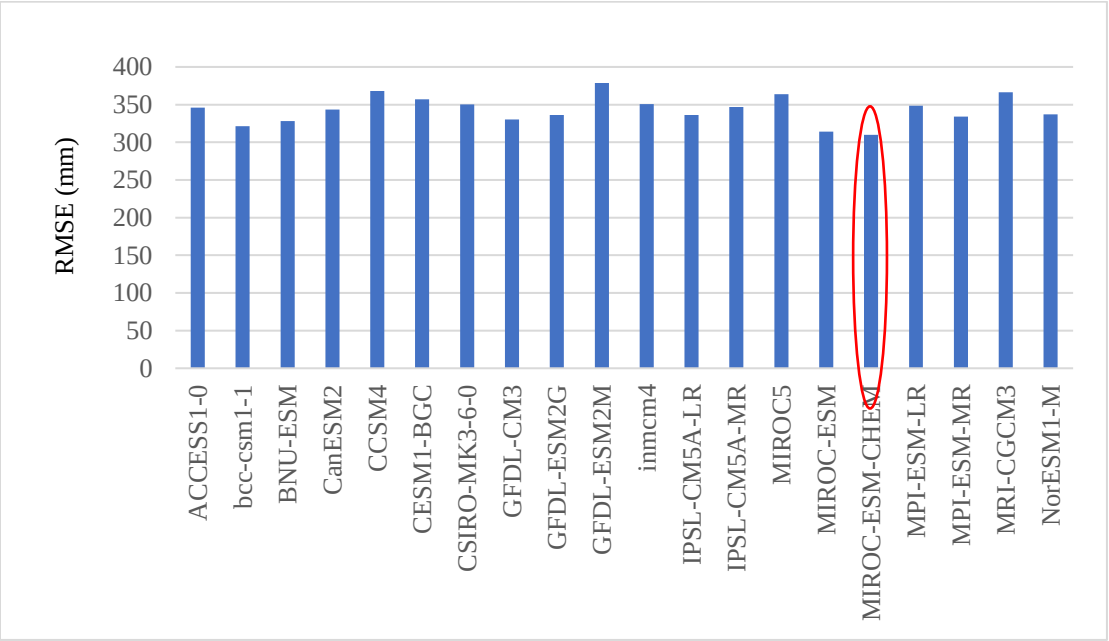

Figure A3. Annual precipitation RMSE between historical observations and GCM output over 1980-2005 for the Middle East region.

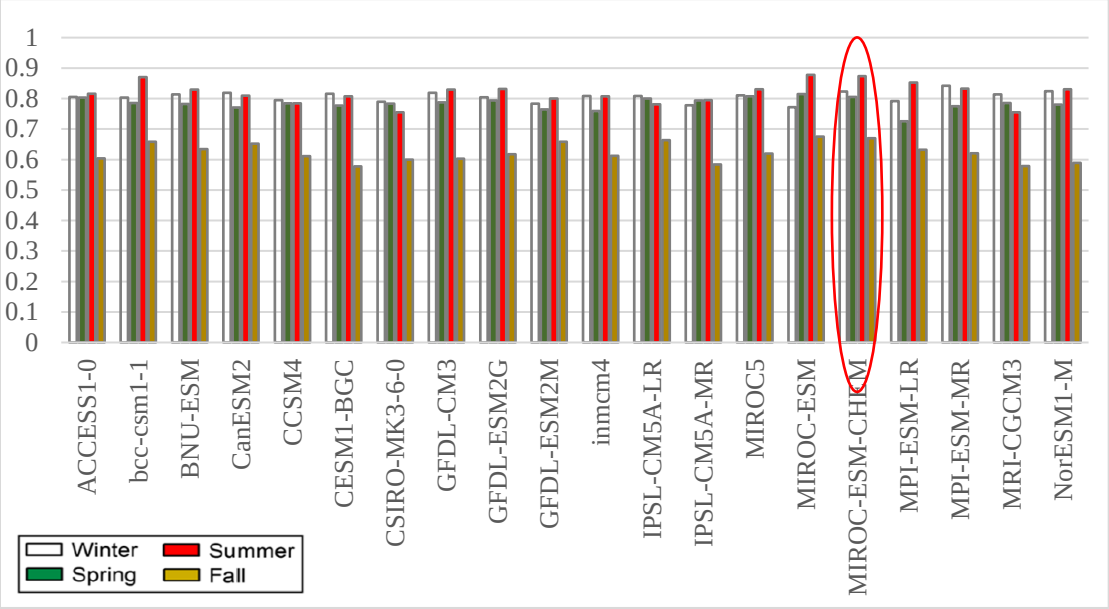

Figure A4. Seasonal precipitation correlations between historical observations and GCM output over 1980-2005 for the Middle East region.

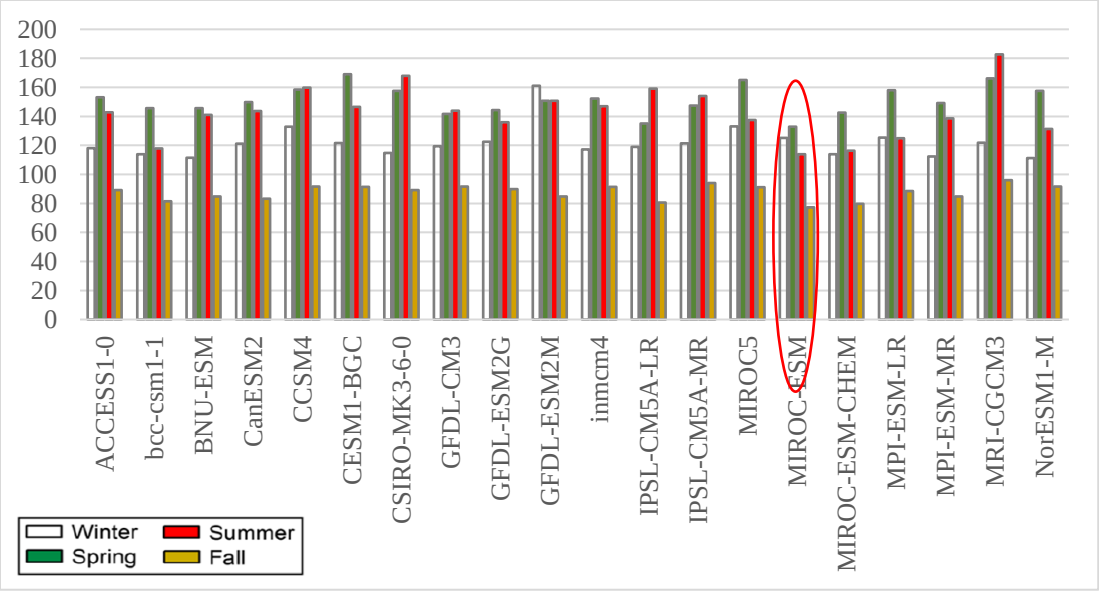

Figure A5. Seasonal precipitation RMSE between historical observations and GCM output over 1980-2005 for the Middle East region (mm).

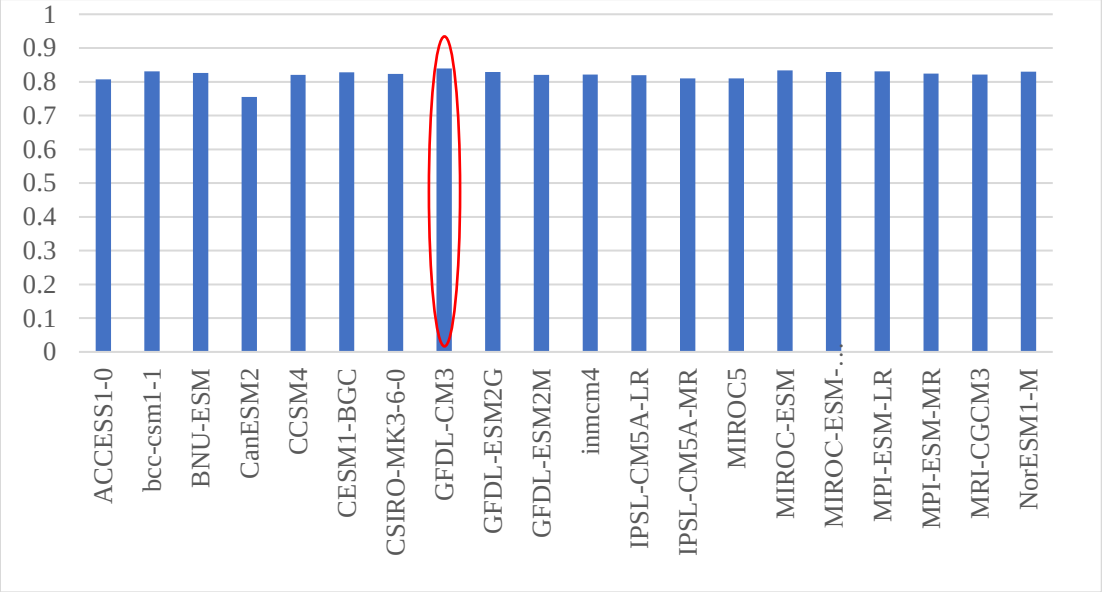

Figure A6. The average length of the dry spell per growing period correlations between historical observations and GCM output over 1980-2005 for the Middle East region.

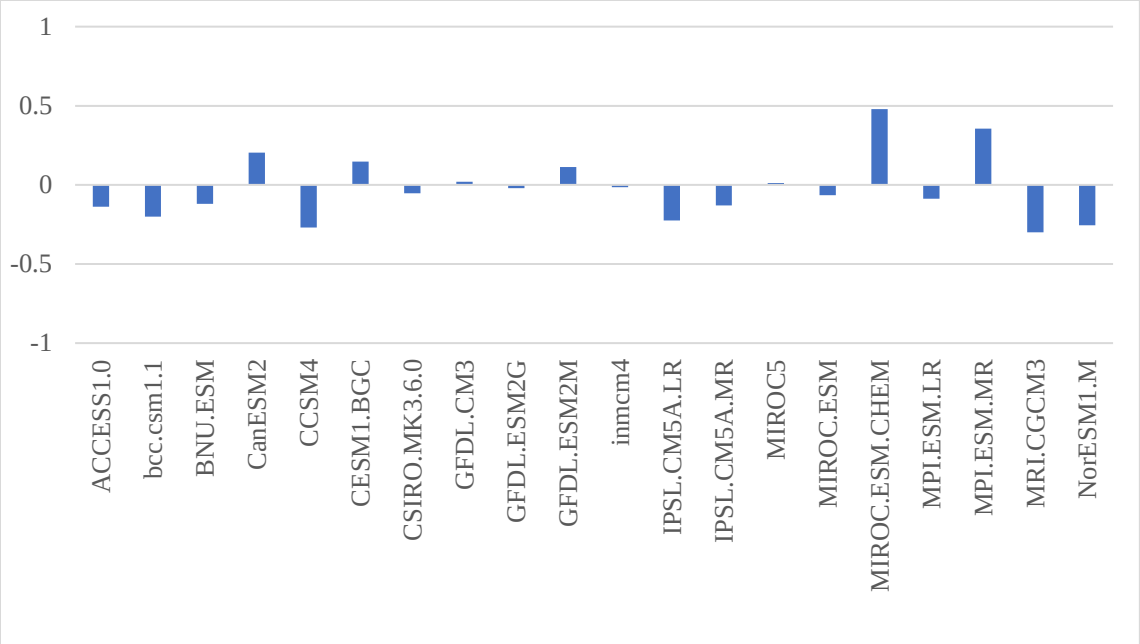

Figure A7. The average length of the dry spell per growing period correlations between historical observations and GCM runs over 1980-2005 for Tigris-Euphrates RB in AEZ8 in Iraq.

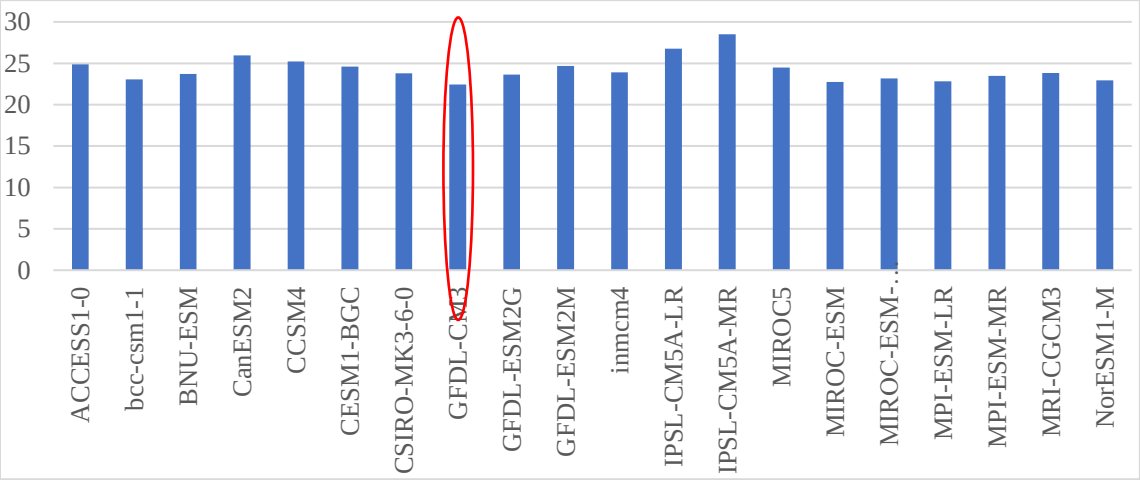

Figure A8. The average length of the dry spell per growing period RMSE between historical observations and GCM runs over 1980-2005 for the Middle East region (days).

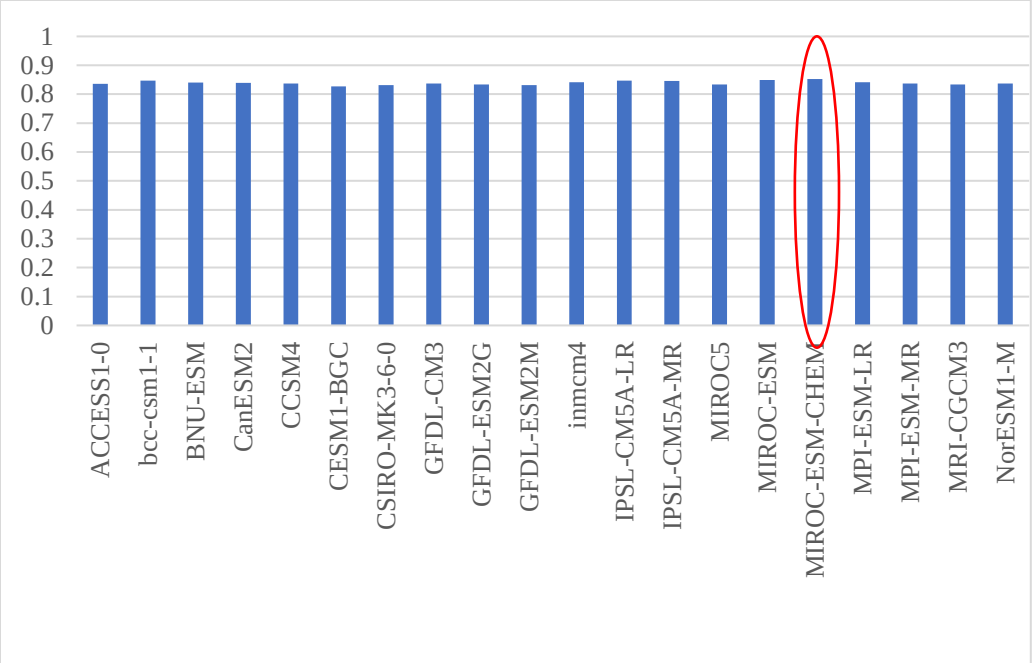

Figure A9. The maximum length of the dry spell per growing period correlations between historical observations and GCM output over 1980-2005 for the Middle East region.

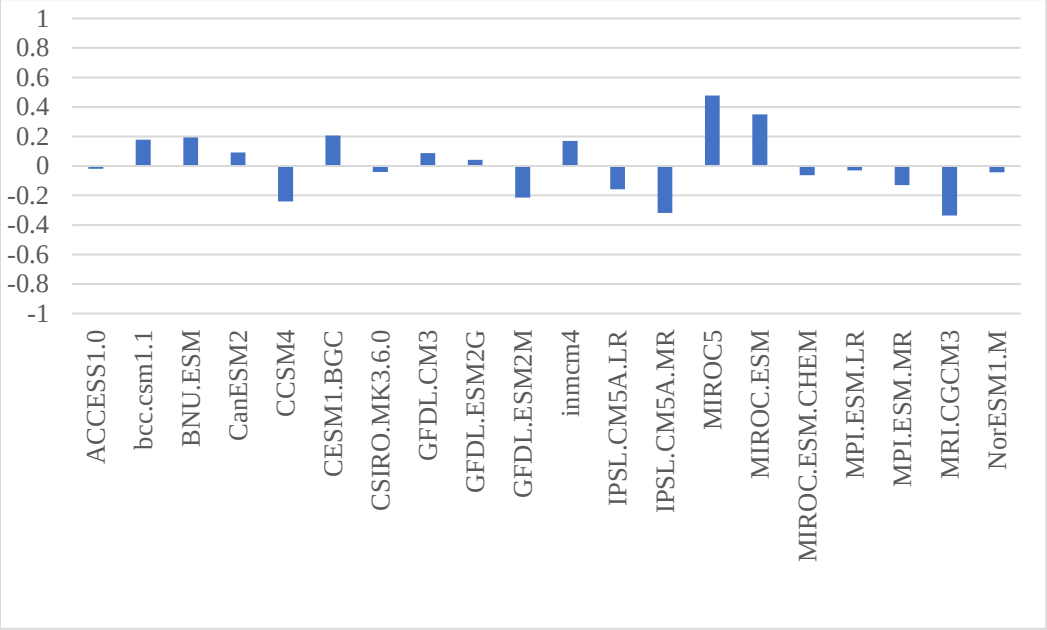

Figure A10. The maximum length of the dry spell per growing period correlations between historical observations and GCM output over 1980-2005 Tigris-Euphrates RB in AEZ8 in Iraq.

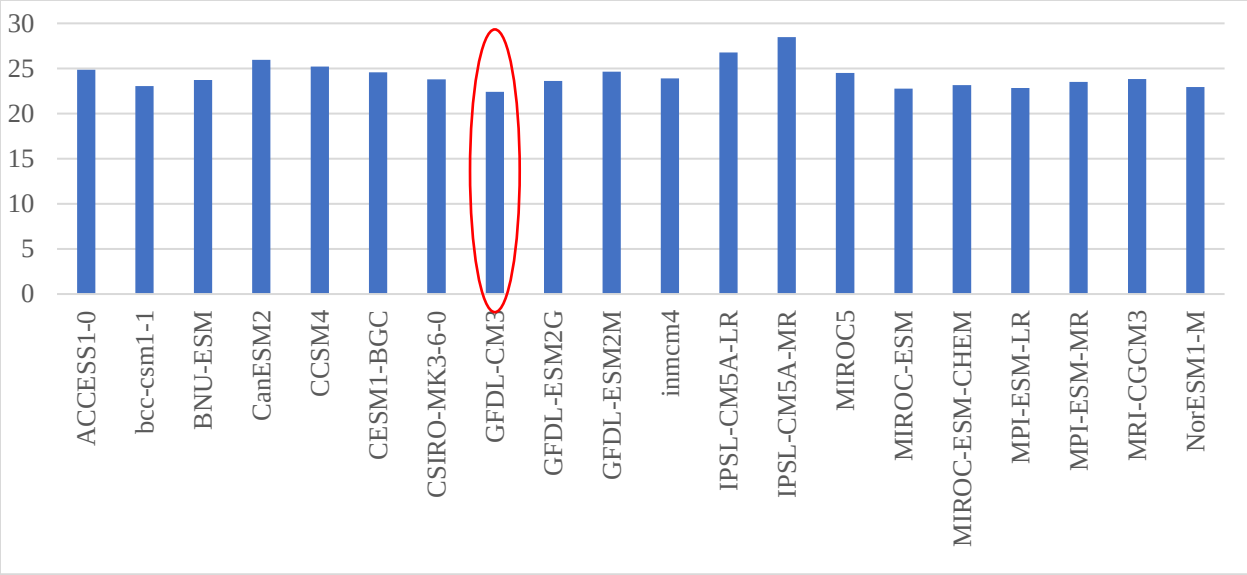

Figure A11. The maximum length of the dry spell per growing period RMSE between historical observations and GCM output over 1980-2005 for the Middle East region (days).

One of the data sources we use to obtain projections of future climate is NASA Earth Exchange Global Daily Downscaled Projections (NEX-GDDP-CMIP6) (Thrasher, B. et al. 2021; 2022). NEX-GDDP-CMIP6 includes the outputs of many GCM models. Ideally, we would like to run the hydrological model with each GCM output. However, this would require very large computing resources. Using the results of the correlation and RMSE analysis above, and given that MIROC-ESM-CHEM is not among CMIP6 models, we have chosen MIROC family model MIROC-ES2L as a source of future climate projections.

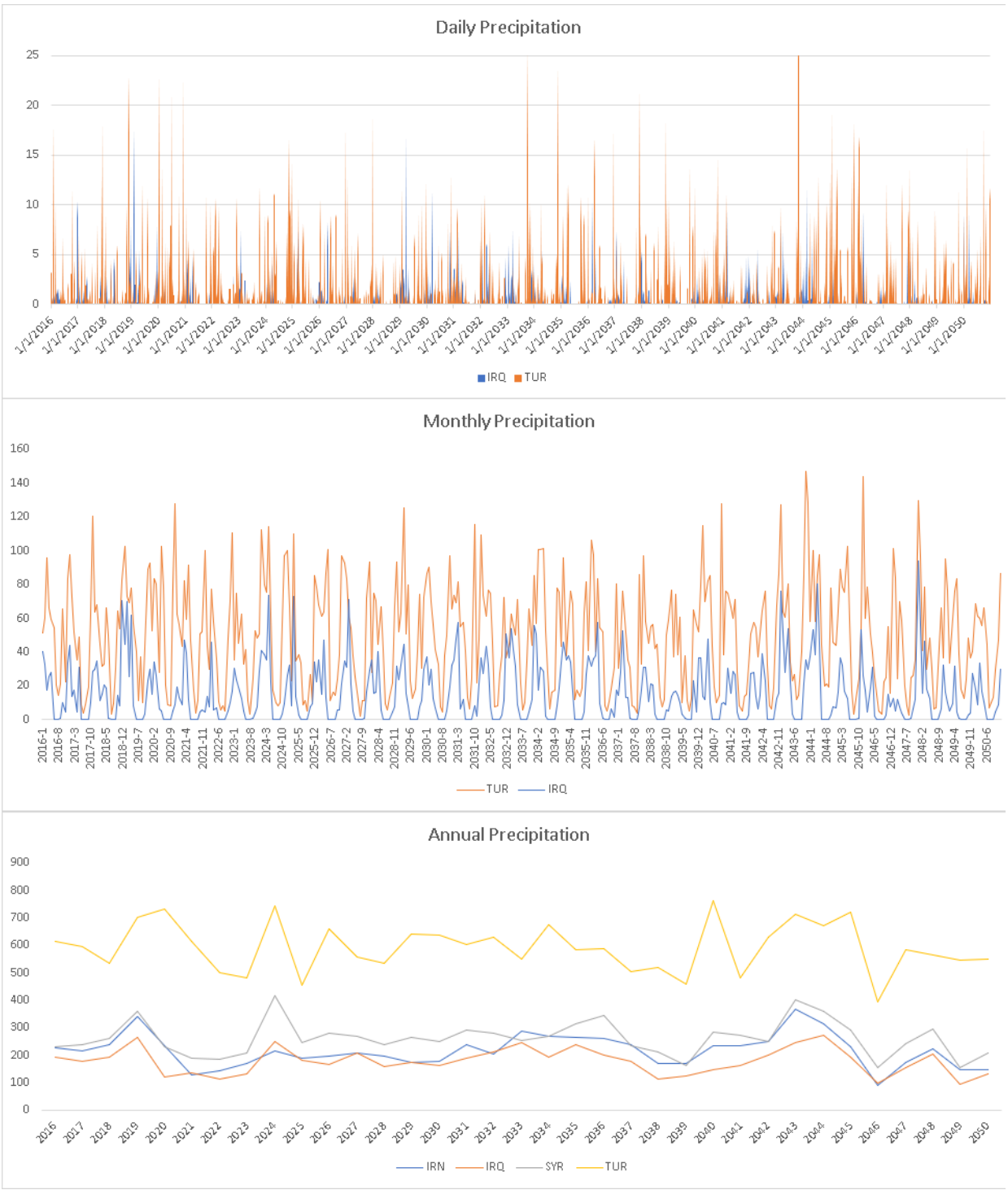

Figure A12. Precipitation for selected countries based on the daily output of the MIROC-ES2L model from NEX-GDDP-CMIP6 with SSP5-8.5

Appendix B

Table B1. Impacts of reduction in water supply driven by RCP8.5 climate scenario and assumed changes in total factor productivity on crop output in the Middle East by crop and country/region, % change.

	Paddy_Rice	Wheat	CrGrains	Oilseeds	Sugar_Crop	Vegetables	Fruits_Oth
With climate impacts on crop yields							
Water scarcity is based on ensemble input in the hydrological model							
Iran	-2.9	-6.1	-9.1	-4.0	-3.2	-3.0	-3.4
Iraq	-7.8	-13.0	-4.2	-10.7	-1.4	-12.8	-10.5
Jordan	0.0	-23.1	-9.3	2.2	0.1	-0.3	-1.2
Lebanon	-6.1	-26.3	-12.3	4.1	-0.5	-1.0	-2.3
Saudi	3.1	0.4	-2.7	-0.1	-0.8	-3.1	-1.7
Syria	0.0	-8.6	-10.2	-1.5	-3.0	-3.8	-5.4
Turkey	-16.7	-21.3	-5.9	-5.7	-2.8	-5.6	-8.2
RME	-5.8	-34.9	-10.1	14.9	-0.6	-0.3	0.0
Water scarcity is based on MIROC-ES2L input in the hydrological model							
Iran	-7.0	-12.9	-17.0	-13.5	-10.1	-8.7	-9.7
Iraq	-12.5	-19.9	-6.9	-16.2	-3.5	-18.0	-14.7
Jordan	0.0	-28.1	-13.0	0.5	-0.8	0.3	-0.7
Lebanon	-5.1	-25.9	-12.6	3.2	-1.6	-0.8	-2.2
Saudi	4.3	1.0	-3.7	0.0	0.1	-3.7	-1.7
Syria	0.0	-13.4	-15.0	-7.7	-6.1	-6.5	-9.0
Turkey	-32.9	-38.1	-15.0	-23.2	-7.0	-14.0	-20.7
RME	-6.2	-35.1	-10.9	15.3	-1.2	-0.4	0.0
Without climate impacts on crop yields							
Water scarcity is based on ensemble input in the hydrological model							
Iran	-1.5	-2.6	-3.0	-3.6	-2.4	-1.7	-2.0
Iraq	-5.8	-6.4	-3.6	-11.2	-1.9	-12.7	-10.8
Jordan	0.0	-6.6	-3.6	-2.0	-1.0	0.0	-1.0
Lebanon	0.7	-0.8	-0.6	-2.2	-1.3	-1.0	-2.3
Saudi	0.6	0.1	-2.8	-0.1	0.2	-3.1	-1.7
Syria	0.0	-4.4	-4.7	-5.6	-2.7	-2.6	-4.0
Turkey	-10.8	-13.8	-5.5	-11.3	-2.5	-5.5	-8.2
RME	-0.9	-0.3	-1.3	0.8	-0.8	-0.8	-0.9
Water scarcity is based on MIROC-ES2L input in the hydrological model							
Iran	-5.5	-9.3	-10.8	-12.5	-9.0	-7.2	-8.1
Iraq	-10.4	-13.5	-6.3	-16.9	-4.0	-18.2	-15.2
Jordan	0.0	-12.8	-7.5	-3.8	-1.9	0.4	-0.7
Lebanon	1.8	-0.6	-0.9	-3.1	-2.4	-0.8	-2.3
Saudi	1.6	0.7	-3.7	0.0	1.0	-3.7	-1.7
Syria	0.0	-9.2	-9.9	-11.6	-5.9	-5.6	-7.9
Turkey	-27.8	-33.0	-14.4	-26.8	-6.7	-13.9	-20.6
RME	-1.3	-0.8	-2.2	0.8	-1.4	-1.0	-0.8

Appendix C:

The hydrological model's projections are used to evaluate future water scarcity. In this appendix, we present important features of the hydrological model and explain how water scarcity shocks are calculated. First, it is important to note that the hydrological model takes care of water stress on crops, not heat stress on crops. Therefore, this model determines additional water needed to maintain the irrigated area with no reduction in yield due to water stress. Second, the additional water withdrawal will not necessarily be all used by crop sectors. Water use efficiency is usually very low in the Middle East. This means that a relatively large portion of the additional water withdrawal may be lost through the irrigation system. Third, with less precipitation (less rain) more water is needed for irrigation on the same area of irrigated land. Finally, the hydrology model traces water withdrawal in three categories: Surface Water (SW), Shallow Groundwater (GW), and Unsustainable Groundwater (UGW). With less precipitation, less SW and GW will be available, which will be compensated by larger withdrawals from UGW. Total Water Withdrawal (WW) is the sum of three types of water withdrawals. The changes in the first two categories do not represent water scarcity. The index of water scarcity is defined as:

S=(-(UGW2-UGW1)/WW1)*100

Here "1" and "2" represent 2016 and 2050. We use the hydrological model projections to calculate the magnitude of water scarcity for each river basin and country. To accomplish this task, we used the following steps:

- For a given combination of climate scenario and data source, annual projections for WW and UWG were determined using the hydrological model from 2016 (base year) to 2054 (last year of the simulation).
- Linear trends have been determined for WW and USW using simple regression.

- Using the estimated trend lines, quantities of WW and UGW were determined for 2016 and 2050.
- Percent changes in water scarcity were calculated using the formula defined above in combination with the estimated quantities determined in the previous step.